Bitumen II from the Paleoproterozoic *Here's Your Chance* Pb/Zn/Ag deposit: implications for the analysis of depositional environment and thermal maturity of hydrothermally-altered sediments

Alex I. Holman [a], Kliti Grice [a]*, Caroline M. B. Jaraula [a], Arndt Schimmelmann [b]

[a] *Western Australia Organic and Isotope Geochemistry Centre, Department of Chemistry, Curtin University, GPO Box U1987 Perth, WA 6845, Australia*

[b] *Department of Geological Sciences, Indiana University, 1001 East 10th Street, Bloomington, IN 47405-1405, USA*

* Corresponding author. Tel.: +61(0) 8 9266 2474; fax: +61(0) 8 9266 2300.

E-mail address: K.Grice@curtin.edu.au (Kliti Grice).

Abstract

The formation of sedimentary exhalative (SEDEX) Pb/Zn deposits is linked to ocean euxinia, but recent evidence suggests that ferruginous conditions may have dominated the deep ocean during the Middle Proterozoic, a maximum period for SEDEX distribution. Biomarkers of sulfate-reducing and sulfide-oxidising bacteria are valuable indicators of euxinic conditions in such settings. Organic matter (OM) from SEDEX deposits is often affected by alteration and/or migration, but OM entrapped within the kerogen/mineral matrix (Bitumen II) may be less affected than the freely-extractable OM (Bitumen I). We analysed Bitumen II from the Paleoproterozoic *Here's Your Chance* (HYC) Pb/Zn/Ag deposit to find evidence of euxinic conditions in the depositional environment. *n*-Alkane distributions in Bitumen II are markedly distinct from previously-reported Bitumen I. Bitumen II contains long-chain *n*-alkanes (up to C_{36} or C_{38}) and a strong even-over-odd distribution in a number of samples, which are 4 to 7‰ depleted in ^{13}C compared to *n*-alkanes in Bitumen I and verified as indigenous by comparison with $\delta^{13}C$ of isolated kerogen. These features are interpreted as evidence of sulfate-reducing and sulfide-oxidising bacteria, confirming that HYC was deposited under euxinic conditions. Bitumen II has the potential to reveal information from OM that is degraded and/or overprinted in Bitumen I. Commonly-used methylphenanthrene maturity ratios give conflicting information as to the relative maturity of Bitumens I and II. Bitumen I contains a far higher proportion of methylated

phenanthrenes than Bitumen II. As Bitumen II is sequestered within the kerogen/mineral matrix it may have restricted access to the 'methyl pool' of organic compounds that can donate methyl groups to aromatic hydrocarbons. Parameters that include both phenanthrene and methylphenanthrenes do not appear suitable to compare maturity of Bitumen I and II; hence there is no clear evidence that Bitumen II is of lower thermal maturity than Bitumen I.

1. Introduction

Sedimentary exhalative (SEDEX) deposits are stratiform, sediment-hosted Pb/Zn ore bodies dominated by sulfide minerals. The genetic models of these deposits are complex and have been extensively reviewed (e.g. Large et al., 2005); the general aspects are deposition of Pb and Zn from a hydrothermal brine in rifted sedimentary basins. The occurrence of major SEDEX mineralisation from *ca* 1800 Ma has been linked to the development of widespread oceanic euxinia during the middle Proterozoic (Lyons et al., 2006). Recent evidence however shows that ferruginous conditions may have dominated in the deep ocean during this period, with euxinia being restricted to isolated basins and mid-depth coastal waters (Poulton et al., 2010; Planavsky et al., 2011). Organic biomarkers are a reliable proxy for the presence of euxinic conditions. For example the breakdown products of carotenoid pigments produced by green and purple sulfur bacteria indicate

64 photic zone euxinia in ancient marine systems (Brocks et al., 2005; Grice et
65 al., 2005).

66 Organic compounds are also useful as indicators of thermal maturity,
67 providing a valuable indication of fluid temperature for deposits which lack
68 fluid inclusions (e.g. Large et al., 2005). SEDEX and other deposits often
69 contain high abundances of polycyclic aromatic hydrocarbons (PAHs)
70 (Püttmann et al., 1989; Williford et al., 2011), highly condensed aromatic
71 compounds made up of two or more benzene rings. Low-molecular-weight
72 PAHs such as naphthalene and phenanthrene are almost ubiquitous in
73 sediments. They can be formed through diagenetic alteration of natural
74 organic precursors (e.g. Wakeham et al., 1980a; Grice et al., 2007; Grice et
75 al., 2009) or by combustion of biomass (Venkatesan and Dahl, 1989;
76 Nabbefeld et al., 2010a) and fossil fuels (Wakeham et al., 1980b). High-
77 molecular-weight PAHs are found in high abundance in high-temperature
78 (> 300 °C) marine hydrothermal vents (Kawka and Simoneit, 1990), where
79 they are generated by the addition of C_2 or C_2H_4 units to existing aromatic
80 compounds (Stein, 1978). Methylated PAHs are produced by geosynthetic
81 methylation reactions in sediments (Voigtmann et al., 1994). PAHs
82 methylated in ß positions are more thermodynamically stable than those in
83 α positions (Szczerba and Rospondek, 2010), and hence the ratios of ß to α
84 isomers are frequently used as indicators of thermal maturity. Ratios of
85 methylphenanthrene (MP) isomers include the methylphenanthrene index

86 (MPI-1) and methylphenanthrene ratio (MPR) (Radke et al., 1982, see Fig 1.
87 for equations).

88 The Mt. Isa-McArthur basin system of Northern Australia is host to
89 five supergiant Proterozoic SEDEX deposits; the most significant
90 accumulation of Pb and Zn in the world (Large et al., 2005). The largest of
91 these deposits is the *Here's Your Chance* (HYC) deposit, hosted in
92 unmetamorphosed carbonaceous and pyritic shales and siltstones of the
93 Barney Creek Formation (BCF). Organic matter (OM) from HYC has been
94 strongly affected by hydrothermal alteration from the mineralising fluid
95 (see Section 2.1) and diagnostic biomarkers have been degraded and
96 possibly overprinted by non-indigenous OM. Traditional extraction
97 techniques can therefore give limited information on the depositional
98 environment and thermal maturity. Removal of silicate minerals from
99 extracted rock powder by digestion with hydrofluoric acid (HF) liberates a
100 second fraction of extractable OM, which is likely to be protected from
101 migration and alteration (Sherman et al., 2007; Nabbefeld et al., 2010b).
102 This fraction is referred to as Bitumen II, whereas the first extract is called
103 Bitumen I. The methods used in this study for the extraction of Bitumen II
104 have been previously reported and validated by Holman et al. (2012). In this
105 study we isolate and analyse Bitumen II from a range of HYC samples in an
106 attempt to distinguish between indigenous and migrated OM and reveal
107 evidence that the deposit was formed in a euxinic environment. A previous
108 report has found that PAH maturity ratios in Bitumen II show different

values than those in Bitumen I (Nabbefeld et al., 2010b), so we also evaluate PAH ratios to determine whether Bitumen II has been protected from thermal alteration.

2. Materials and methods

2.1 The Barney Creek Formation and the Here's Your Chance deposit

The 1640 Ma (Page and Sweet, 1998) carbonaceous, pyritic and tuffaceous shales and siltstones of the Barney Creek Formation (BCF) in the McArthur Basin, Northern Territory, Australia were originally interpreted as a deep marine succession deposited in a reducing environment below the wave base (Bull, 1998). More recently, it has been recognised that these sediments are part of a facies mosaic of time-equivalent shelf, slope and deep-water sediments deposited in a series of tectonically controlled sub-basins (McGoldrick et al., 2010). The BCF has been widely studied as it contains possibly the most well-preserved Proterozoic organic matter (OM) (Summons et al., 1988). BCF black shales generally contain 0.2 to 2 wt.% total organic carbon, and locally greater than 7 wt.% (Powell et al., 1987). Previous studies of low-maturity shales from the Glyde River region of the BCF have found biomarkers of the sulfide-oxidising green and purple sulfur bacteria Chlorobiaceae and Chromatiaceae (Brocks et al., 2005; Brocks and Schaeffer, 2008). These bacteria are known to thrive in marine systems

130 where euxinic conditions persist in the photic zone of the water column (e.g.
131 Summons and Powell, 1987; Grice et al., 2005).

132 The BCF is host to the HYC Pb-Zn-Ag deposit, one of the largest
133 sediment-hosted base metal deposits in the world. The HYC deposit has a
134 total resource of 227 Mt, at 9.25 wt. % Zn, 4.1 wt. % Pb and 41 ppm Ag
135 contained in eight discreet ore lenses (Walker et al., 1977; Large et al.,
136 2005). The deposit is generally considered to have been formed by
137 exhalation of a metal-rich hydrothermal brine into the water column
138 (Croxford, 1968; Ireland et al., 2004a; Large et al., 2005). The OM at HYC
139 has been strongly affected by hydrothermal alteration, but several studies
140 have used OM to investigate the conditions of deposition (Logan et al., 2001;
141 Chen et al., 2003; Williford et al., 2011). HYC *n*-alkanes are enriched in
142 deuterium by 50 to 60‰ compared to those from the unmineralised BCF,
143 indicating isotopic exchange with a D-enriched evaporitic brine (Williford et
144 al., 2011). Williford et al. also presented carbon isotopic data which suggest
145 that a significant quantity of aromatic hydrocarbons were generated in the
146 underlying Wollogorang Fm and transported to the deposit within the
147 mineralising fluid

148 The samples used were collected and analysed by Williford et al.
149 (2011). Five samples of Pb-Zn-Ag sulfide ore were taken from the highly
150 mineralised upper ore body 5 of the deposit (referred to as sample pits 1 to
151 5), plus one non-mineralised shale sample from the underlying W-Fold
152 Shale member, a sequence of red-green shales and siltstones at the basal 10

153 to 15 meters of the BCF at and around the area of the mine (Walker et al.,
154 1977).

155

156 *2.2 Extraction and separation of Bitumen II*

157 The extraction of Bitumen II followed a procedure modified from Robl
158 and Davis (1993) and Nabbefeld et al. (2010b), as detailed by Holman et al.
159 (2012) for the pit 1 sample. The other samples were prepared using the
160 same method. HCl and HF were cleaned prior to use by shaking with
161 dichloromethane (DCM) to remove organic contaminants from the acids.
162 GC-MS analysis (Section 2.4) revealed that saturate and aromatic
163 contaminants were below the limit of detection after cleaning.

164 Extracted rock powder was digested with HCl (1 M) to remove
165 carbonates then placed into clean 50 mL polyethylene centrifuge tubes (5-6
166 g of sample per tube). Equal volumes of concentrated HF (48 wt.%) and
167 Milli-Q purified water were added to the tubes and left to digest (1-2 hours)
168 in an ice bath with regular shaking. The supernatant liquid was then
169 decanted and a second volume of acid-water mixture was added. The tubes
170 were left at room temperature (3-4 hours) with occasional shaking to
171 complete the digestion. The solid residue was then washed (3 ×) with Milli-Q
172 water and freeze dried. The samples had decreased in mass by ca. 50%.

173 After the acid digestion the samples were extracted in a Soxhlet
174 apparatus (72 hours) with 9:1 (v:v) DCM: methanol (MeOH) to extract

175 Bitumen II, replicating the conditions used by Williford et al. (2011) to
176 isolate Bitumen I. Copper turnings (rinsed with DCM and activated with
177 dilute HCl) were added to the flask to remove elemental sulfur. The extract
178 was evaporated to dryness under a stream of warm N_2, dissolved in a
179 minimum amount of DCM and added to the top of a small column (5.5 cm ×
180 0.5 cm i.d.) of silica gel (activated at 160 °C for 24 hrs). The total extract was
181 separated into saturate, aromatic and polar fractions by elution with *n*-
182 hexane, 30 vol.% DCM in *n*-hexane and 1:1 DCM:MeOH respectively. Semi-
183 quantitative analysis of aromatic fractions was done using an internal
184 standard of deuterated *p*-terphenyl.

185

186 *2.3 Isolation of kerogen*

187 Following the extraction of Bitumen II a fraction of each sample was
188 taken for the isolation of kerogen, following the procedure of Nabbefeld et al.
189 (2010b). A small amount of sample was placed into glass centrifuge tubes (<
190 1 g per tube) and shaken with 2-3 mL of saturated aqueous zinc bromide
191 solution ($\rho \approx 2.4$ g mL^{-1}). After centrifugation (2000 RPM, 5 min) the acid-
192 insoluble minerals settled to the bottom of the vial while the isolated
193 kerogen remained floating on or suspended in the ZnBr solution. The liquid
194 was then decanted and diluted with Milli-Q water to allow the kerogen to
195 settle. The kerogen was washed with Milli-Q water (×3) and freeze-dried.

30-50 mg of kerogen was isolated for each sample from 3-5 g of acid-digested rock powder.

2.4 Gas chromatography mass spectrometry (GC-MS)

Saturate and aromatic fractions were analysed by GC-MS using a Hewlett Packard (HP) 6890 gas chromatograph coupled to a HP 5973 mass selective detector, following the procedure of Holman et al. (2012). Fractions were dissolved in *n*-hexane and injected into a split-splitless injector in pulsed splitless mode. A DB5-MS column (Agilent Technologies, 60 m length, 0.25 mm i.d., 0.25 µm film thickness) was used with He as the carrier gas. The GC oven temperature was increased from 40 °C to 310 °C at 3 °C min^{-1} then held isothermally for 30 min. Data were acquired in full scan mode (m/z 50–550).

2.5 Stable carbon isotope analysis

Compound-specific stable carbon isotope ratios ($\delta^{13}C$) of the saturate fractions were measured using a HP 6890 gas chromatograph coupled to a Micromass IsoPrime isotope ratio monitoring mass spectrometer (irm-MS). The GC oven was held at 50 °C for 1 min, increased to 310 °C at 3 °C min^{-1} then held isothermally for 20 min. The GC column was the same as that described in Section 2.4. $\delta^{13}C$ values are reported relative to CO_2 reference

gas calibrated to the Vienna Pee Dee Belemnite (VPDB) scale. Samples were analysed 2 to 5 times each, and standard deviations for measured compounds ranged from 0.2 to 0.5‰. The instrument was calibrated daily with a mixture of compounds of known $\delta^{13}C$ to monitor the precision and accuracy of analysis. The aromatic fractions were of insufficient quantities to perform compound-specific isotope analysis.

Bulk stable carbon isotope ratios of isolated kerogens were measured using a Delta V Plus mass spectrometer connected to a Thermo Flush 1112 elemental analyser via a Conflo IV (Thermo-Finnigan/Germany).

3. Results

3.1 Bitumen II saturated hydrocarbons

Total ion chromatograms (TICs) of Bitumen II saturated hydrocarbon fractions from sample pits 1 and 3, which together exemplify the most important features of all the samples, are displayed in Fig. 2. Samples from pits 1, 5 and the W-Fold Shale show a significant predominance of *n*-alkanes with even carbon numbers, while this pattern is less pronounced in ore from pits 2, 3 and 4. Long-chain *n*-alkanes up to *n*-C_{36} are present in all samples, with *n*-C_{37} and *n*-C_{38} present only in pits 1 and 5. These distributions are characterised by Average Chain Length (ACL) and Carbon Preference Index (CPI), which are presented in Table 1. The ACL in Bitumen II ranges from

238 25.4 to 26.9, which is greater than the Bitumen I ACL of roughly 18
239 (Williford et al., 2011).

240 CPI measures the ratio of *n*-alkanes with odd carbon numbers over
241 those with even carbon numbers, and is calculated here using the formula of
242 Marzi et al. (1993). The Bitumen I *n*-alkanes reported by Williford et al.
243 (2011) show no predominance of odd or even carbon numbers and hence the
244 CPI will approximately equal one. The CPI of Bitumen II from pits 1, 5 and
245 the W-Fold Shale samples range from 0.59 to 0.83, showing a strong
246 prevalence of even-numbered *n*-alkanes that is seen in Fig. 2a. The
247 remaining samples have CPI values much closer to one and show no obvious
248 carbon number preference (Fig. 2b).

249

250 *3.2 Stable carbon isotope analysis*

251 Compound-specific stable carbon isotope ratios for Bitumen II *n*-
252 alkanes and isolated kerogen are listed in Table 1. Values are reported in
253 the ranges C_{16} and C_{18}, and C_{24} to C_{32}, as these were the compounds that
254 were of sufficient abundance to measure $\delta^{13}C$. The $\delta^{13}C$ values of Bitumen II
255 *n*-alkanes (-34.4 to -31.6‰) are 4 to 7‰ lower than those in Bitumen I
256 (Williford et al., 2011). Within Bitumen II the long chain *n*-alkanes (C_{24} to
257 C_{32}) are generally 1 to 3‰ lighter than to C_{16} and C_{18}, although the two
258 values are within error for pit 1 and there was insufficient abundance of *n*-
259 C_{16} and *n*-C_{18} from pit 2 to measure their isotopic composition. Bulk kerogen

$\delta^{13}C$ ranges from -37 to -34.2‰, which is 1 to 4‰ lower than Bitumen II long-chain alkanes. No consistent trend in $\delta^{13}C$ is observed between samples for either *n*-alkanes or kerogen (Fig. 3).

3.3 Bitumen II aromatic hydrocarbons

Quantification of selected PAHs in Bitumen II (reported in ng of compound per g of TOC) is presented in Table 2 along with selected ratios of aromatic compounds. Data from pit 1 have been previously reported (Holman et al., 2012). Several methylphenanthrene ratios are also included from Bitumen I, calculated from data reported by Williford et al. (2011). The amounts of aromatic compounds measured in Bitumen II are commonly 5 to 15% that of Bitumen I. As in Bitumen I there is no clear trend in PAH concentrations from pits 1 to 5.

The methylphenanthrene ratios MPI-1 and MPR are plotted for Bitumens I and II in Fig. 4. Both parameters are designed to be a measure of maturity (Radke et al., 1982), however the relationships between the parameters in Bitumens I and II are distinct. MPI-1 for Bitumen I is consistently significantly higher than in Bitumen II (Fig. 4a), whereas the MPR is generally higher in Bitumen II than Bitumen I (Fig. 4b). These differences may be explained by the increased ratio of phenanthrene to methylphenanthrenes (P/MPs) in Bitumen I (Table 2), indicating that

281 Bitumen I contains a greater proportion of methylated isomers (see Section
282 4.2 for discussion).

283

284 **4. Discussion**

285 *4.1 Sources of saturated compounds*

286 The Bitumen II *n*-alkanes reported in this study differ from those
287 previously found in Bitumen I in three main aspects: a marked
288 predominance of even carbon numbers in three out of six samples (Fig. 2),
289 the presence of long-chain alkanes up to C_{38}, and reduced $\delta^{13}C$ values of -34
290 to -31‰ (Fig. 3). These features have not previously been observed together
291 in samples from HYC. Alkane distributions previously reported from HYC
292 Bitumen I have been limited to C_{32} or C_{33}, with $\delta^{13}C$ between -30 and -27‰
293 (Logan et al., 2001; Williford et al., 2011). Logan et al. (2001) observed *n*-
294 alkanes with a strong even-over-odd distribution in highly mineralised
295 samples from ore body 2, however there is evidence that these samples were
296 contaminated with hydrocarbons from plastic sample bags (Grosjean and
297 Logan, 2007) and thus results from this study should be treated with
298 caution.

299 The significant differences between the *n*-alkanes in Bitumens I and II
300 may be due to a different source of OM, a difference in the response to
301 hydrothermal alteration, or a combination of both. *n*-Alkanes from
302 Proterozoic sediments are typically enriched 2 to 3‰ in ^{13}C compared to the

303 source kerogen (Logan et al., 1995). Carbon isotopic data (Table 1) shows
304 that *n*-alkanes in HYC Bitumen II bear this exact relationship with the
305 isolated kerogens from HYC. These data strongly suggest that Bitumen II *n*-
306 alkanes are indigenous to HYC, in accordance with the contention that
307 Bitumen II is less likely to be overprinted by migrated OM (Sherman et al.,
308 2007). It was proposed by Williford et al. (2011) that aromatic hydrocarbons
309 in Bitumen I were transported to HYC from the underlying Wollogorang
310 Fm. The similar $\delta^{13}C$ of aromatics and *n*-alkanes in Bitumen I (Williford et
311 al., 2011) suggest that saturated compounds may also have been
312 transported. The migration of non-indigenous *n*-alkanes would obscure the
313 even-over-odd distribution, resulting in the more typical Proterozoic
314 distribution of Bitumen I.

315 A strong even-over-odd preference of *n*-alkanes is uncommon in the
316 geological record, but has been observed in a variety of marine sediments
317 (e.g. Dembicki Jr et al., 1976; Simoneit, 1994). George et al. (1994) studied
318 solid bitumens from the *ca* 1400 Ma Roper Group in the McArthur Basin.
319 Several of these samples displayed a slight even-over-odd *n*-alkane
320 predominance. These alkanes were also depleted in ^{13}C compared to those
321 which did not show an even-over-odd distribution. It was concluded that
322 solid bitumens in the Roper Group incorporate multiple sources of organic
323 input, including one which is isotopically light and contains a high
324 proportion of even-numbered alkanes (George et al., 1994). Possible origins
325 of this input were not discussed in detail, but a number of studies have

connected similar *n*-alkane distributions with the presence of sulfate-reducing and sulfide-oxidising bacteria. For instance, a strong predominance of isotopically light even-numbered *n*-alkanes in microbial mat facies of the Neoproterozoic Centralian Super-basin was ascribed to the activity of purple or colourless sulfur bacteria (Logan et al., 1999). A recent report of a 380 Ma fossil invertebrate preserved within a carbonate concretion in the Canning Basin, Western Australia also showed *n*-alkanes with a pronounced even-over-odd distribution in the desulfurised fossil extract, along with ^{13}C-depleted long-chain *n*-alkanes in the fossil nucleus and carbonate matrix (Melendez et al., 2013). Biomarker and isotopic evidence revealed the strong activity of sulfate reducing bacteria and green sulfur bacteria (Chlorobi) in conditions of photic zone euxinia at the time the fossil was preserved.

Analyses of lipids from microbial cultures have shown that the phototrophic sulfur bacterium Chlorobi produces *n*-alkanes with a marked even-over-odd distribution over the range C_{15} to C_{28}, while the sulfate-reducing bacterium *Desulfovibrio Hildenborough* produces a similar but less pronounced distribution over the range C_{19} to C_{31} (Han and Calvin, 1969). Sulfate reducing bacteria are known to generate long-chain lipids: *D. desulfuricans* produces *n*-alkanes predominantly in the range C_{25}-C_{35} (Ladygina et al., 2006), while long chain fatty acids up to C_{34} were found in *Desulfotomaculum* (Řezanka et al., 1990). Both sulfate-reducing bacteria and phototrophic sulfur bacteria produce lipids that are significantly

depleted in ^{13}C compared to the biomass. Lipids from sulfate reducing bacteria were found to be depleted 4 to 17‰ (Londry et al., 2004) and lipids from purple sulfur bacteria were depleted by up to 20‰ (Madigan et al., 1989).

The distinctive even-over-odd distribution of *n*-alkanes in Bitumen II was likely generated by phototrophic sulfur bacteria, while the ^{13}C-depleted long-chain *n*-alkanes in Bitumen II indicate sulfate-reducing bacteria. Their presence in Bitumen II, closely associated with the kerogen/mineral matrix, implies that these bacteria were present at the time of ore deposition. This evidence is consistent with deposition under euxinic conditions, as required for the formation and preservation of large-scale sulfide deposits (Lyons et al., 2006). The extent of euxinia into the photic zone is evidenced by the presence of phototrophic sulfur bacteria. The results fit the generally-held model in which a metal-rich hydrothermal brine was vented into the basin, reacting with bacterially-produced sulfide to form fine-grained base metal sulfides (Ireland et al., 2004b; Large et al., 2005). Recent findings of widespread ferruginous conditions in the McArthur Basin (Planavsky et al., 2011) suggest that euxinia was restricted to localised settings, such as the HYC sub-basin (McGoldrick et al., 2010) and the Glyde River region studied by Brocks et al. (2005). A increased supply of sulfate to a basin would promote euxinia over ferruginous conditions (Poulton et al., 2010). Sulfate carried by the oxidised hydrothermal fluid (Cooke et al., 2000) may have contributed to the development of euxinic conditions during the deposition

372 of HYC. It is notable that the evidence of euxinia is seen only in Bitumen II;
373 the distinctive features from sulfate-reducing and sulfide-oxidising bacteria
374 have been removed from Bitumen I by the actions of hydrothermal
375 alteration and migration of non-indigenous OM.

376

377 *4.2 Aromatic hydrocarbons in Bitumens I and II*

378 The aromatic fractions of both Bitumens I and II are dominated by
379 PAHs. The distribution of PAHs (Fig. 2c) follows the most
380 thermodynamically favourable pathway for the creation of condensed
381 aromatic molecules (Stein, 1978) and is typical of those found in
382 hydrothermal systems (e.g. Kawka and Simoneit, 1990). The high
383 abundance of PAHs indicates that Bitumen II, like Bitumen I, has
384 experienced significant hydrothermal alteration. The quantity of PAHs in
385 Bitumen II (Table 2) is much lower than found in Bitumen I (Williford et al.,
386 2011). This could indicate that Bitumen II has been partially shielded from
387 alteration, although it also likely reflects the small amounts of OM available
388 within the kerogen/mineral matrix.

389 A variety of parameters have been developed to evaluate thermal
390 maturity based on the ratios of various methylated isomers of PAHs. Ratios
391 based on methylphenanthrene (MP) isomers have been found in a study of
392 the McArthur Basin to be sensitive to changes in maturity throughout the
393 oil window (George and Ahmed, 2002). Two common MP ratios, MPI-1 and

MPR are shown in Fig. 3 for both Bitumens I and II. The value of MPI-1 in Bitumen I exceeds that of Bitumen II in every sample. If MPI-1 is taken to be a true indicator of maturity this would indicate that Bitumen I is of higher maturity than Bitumen II, suggesting that Bitumen II has been protected from thermal alteration. A different relationship however is observed for MPR. The values for Bitumens I and II are similar, and in some samples Bitumen II exceeds Bitumen I. Both parameters are expected to be indicative of maturity (Radke et al., 1982) but it is apparent that other factors are affecting the behaviour of these two ratios. Williford et al. (2011) proposed that PAHs in Bitumen I were generated at high temperatures (> 250 °C) in the underlying Wollogorang Fm, whereas Bitumen II is likely indigenous to HYC and has experienced temperatures of less than 200 °C (Cooke et al., 2000; Large et al., 2005). The different thermal histories are consistent with the increased MPI-1 values in Bitumen I but cannot explain why MPR is often greater in Bitumen II. Notably this is not the first study that has reported such behaviour. In a study of marine sediments from multiple locations spanning the Permian/Triassic boundary by Nabbefeld et al. (2010b) the same relationships were found. MPI-1 is consistently greater in Bitumen I but the ß/α MP ratio, which is similar to MPR but includes all four isomers rather than only 2- and 1-MP, is frequently greater in Bitumen II. The samples analysed by Nabbefeld et al. are of greatly different age and thermal history to those from this study, hence it appears that the

416 relationships between MPI-1 and MPR are not unique to HYC but rather
417 are a result of fundamental differences between Bitumens I and II.

418 The major difference between MPI-1 and the MPR or ß/α MP ratio is
419 that the unmethylated phenanthrene is included in the denominator of
420 MPI-1 but does not appear in the other ratios. Fig. 5 shows that Bitumen II
421 contains far higher proportions of phenanthrene than Bitumen I.
422 Phenanthrene is more abundant than the MPs in Bitumen II for all samples
423 except the W-Fold Shale, but in Bitumen I it is less abundant than most or
424 all of the MP isomers. The inclusion of phenanthrene in the denominator of
425 MPI-1 causes this ratio to give much lower values for Bitumen II. Higher
426 proportions of phenanthrene in Bitumen II were reported by Nabbefeld et
427 al. (2010b), who also observed that Bitumen II contained a greater
428 proportion of ß methylated isomers compared to Bitumen I. The relationship
429 between ß and α isomers is less consistent in HYC, and the proportion of ß to
430 α isomers appears similar in Bitumens I and II.

431 The increased proportion of phenanthrene in Bitumen II from multiple
432 locations and maturities implies that the cause of the increase is unrelated
433 to location or thermal history. Nabbefeld et al. (2010b) suggest that
434 phenanthrene is preferentially preserved in Bitumen II as it is more stable
435 than the MPs, just as the more stable ß-isomers are preserved over the α-
436 isomers. Comparisons of thermodynamic properties of both phenanthrene
437 and MPs, either experimental or theoretical, are rare, and the relative
438 stabilities are strongly dependant on redox conditions (Püttmann et al.,

439 1989; Dick et al., 2013). Regardless of their relative stabilities it is not clear
440 why phenanthrene should be preferentially retained in Bitumen II over the
441 MPs. Evidence for the retention of the more stable ß-MPs is limited in HYC,
442 but is seen to a greater extent in the results of Nabbefeld et al. (2010b).
443 Previous studies have explained the retention of ß-isomers in coals not by
444 thermodynamic stability but by a 'molecular sieve' effect whereby larger
445 molecules are trapped by pores in the coal structure (Vahrman and Watts,
446 1972). This effect does not explain the retention of the less bulky
447 unmethylated molecule. In a study of the chromatographic behaviour of
448 organic compounds moving through a column of montmorillonite clay,
449 Brothers et al. (1991) found that 2-MP appears to be more strongly adsorbed
450 to the clay than P. This is the opposite effect to that seen in Bitumen II.
451 Studies of the relative adsorption behaviour of phenanthrene and MP are
452 limited, but the available evidence does not seem to support the preferential
453 retention of phenanthrene within the kerogen/mineral matrix.

454 An alternative explanation for the high proportion of phenanthrene in
455 Bitumen II is that the MP isomers are prevented from forming within the
456 kerogen/mineral matrix. MPs in sediments are generated by geosynthetic
457 reactions in which methyl groups are added to unmethylated phenanthrene
458 (Voigtmann et al., 1994). Methylation of phenanthrene has been achieved in
459 the laboratory under moderate temperature conditions in the presence of a
460 clay catalyst, but requires the addition of a methyl donor such as methane
461 (Voigtmann et al., 1994) or existing methylated aromatic compounds

462 (Alexander et al., 1995). A hydrous pyrolysis study found that phenanthrene
463 alone does not undergo methylation even with prolonged heating, but
464 significant methylation occurs with the addition of formic acid (McCollom et
465 al., 1999). From these results it can be inferred that MPs will only form
466 when other organic compounds are present that are able to donate methyl
467 groups. This was recognised by van Aarssen et al. (1999) who proposed the
468 concept of a 'methyl pool' that can be accessed by all aromatic compounds in
469 the sediment. Compounds that are preserved within the kerogen/mineral
470 matrix as part of Bitumen II may have restricted access to the methyl pool
471 and thus display reduced levels of methylation. It has been demonstrated
472 that phenanthrene that is intercalated in clay minerals is significantly less
473 available to biodegrading microorganisms (Theng et al., 2001), and it is
474 feasible that it would experience reduced access to the methyl pool as well.
475 This mechanism can explain the increased proportion of phenanthrene in
476 Bitumen II from both this study and Nabbefeld et al. (2010b).

477 Oxidation state can also affect the proportions of phenanthrene and
478 MPs. A study of the Kupferschiefer deposit (southwest Poland) found
479 increased proportions of phenanthrene in zones of higher oxidation state
480 (Püttmann et al., 1989). PAHs in Bitumen I are believed to have been
481 transported by a fluid that was likely oxidised (Cooke et al., 2000), hence the
482 low proportions of phenanthrene in Bitumen I suggest that redox is not a
483 significant control at HYC.

MPI-1 is commonly used to indicate thermal maturity, but results from this study have shown that the parameter can be heavily influenced by factors that affect the methylation of P. Prior reports have noted that MPI-1 is also strongly influenced by demethylation reactions that occur at high temperatures (Garrigues et al., 1990). The inclusion of phenanthrene in the denominator of MPI-1 means that this ratio is not simply an indicator of maturity, but also reflects the source of OM and the degree of methylation. As such MPI-1 is not a suitable parameter to compare the maturity of Bitumens I and II. Ratios such as MPR, which are based only on MP isomers, are perhaps better suited as indicators of maturity alone. As MPR from Bitumens I and II is generally similar it appears that the two extracts are of approximately equal maturity, and there is no conclusive evidence from MP ratios in this study that Bitumen II is significantly protected from thermal alteration. These results do not support a high-temperature origin for Bitumen I PAHs, as proposed by Chen et al. (2003), although the isotopic evidence for migration of hydrocarbons is strong (Section 4.1).

5. Conclusions

Organic matter at HYC has experienced significant hydrothermal alteration, but Bitumen II may be protected from alteration and migration. Bitumen II prepared from HYC samples reveals highly distinct distributions of saturated and aromatic compounds. Bitumen II *n*-alkanes show a

predominance of even carbon numbers, a preservation of long-chained *n*-alkanes up to C_{38} and a marked depletion in ^{13}C. These features are indicative of strong contribution from sulfate-reducing and sulfide-oxidising bacteria. Comparison with $\delta^{13}C$ of isolated kerogen confirms that *n*-alkanes in Bitumen II are indigenous to HYC, indicating that the deposit formed under euxinic conditions. This evidence supports the generally-held model whereby lead and zinc reacted in the water column with sulfide produced by bacterial sulfate reduction. Bitumen II appears useful in the study of environments that have experienced significant alteration and/or migration, where diagnostic features in Bitumen I have been destroyed or overprinted.

Bitumens I and II both contain high abundances of PAHs. The common maturity parameters MPI-1 and MPR display inconsistent results, with MPI-1 greater in Bitumen I but MPR often greater in Bitumen II. This behaviour is due to the far higher proportion of phenanthrene in Bitumen II compared to Bitumen I. We believe that this is a fundamental property of Bitumen II resulting from restricted access to the 'methyl pool' that contributes to methylation reactions. As MPI-1 is so heavily affected by access to the methyl pool it is not a suitable parameter for comparing the thermal maturity of Bitumens I and II.

Acknowledgements

All authors acknowledge the CSIRO Flagship Collaboration Fund Cluster for Organic Geochemistry of Mineral Systems led by Curtin University. A.H. thanks Curtin University for an Australian Postgraduate Award and CSIRO for a top-up scholarship. The Institute for Geoscience Research (TIGeR) and the John de Laeter Centre for Isotope Research provided additional funding. The authors thank Geoff Chidlow and Peter Sauer for GC-MS technical support, Stephen Clayton for GC-irMS technical support, and Grzegorz Skrzypek for bulk kerogen $\delta^{13}C$ measurements. Peter McGoldrick, an anonymous reviewer and Associate Editor Thomas Wagner provided helpful reviews, and Chris Yeats, Jochen Brocks and Katy Evans gave comments on earlier versions of the manuscript.

References

Alexander R., Bastow T. P., Fisher S. J. and Kagi R. I. (1995) Geosynthesis of organic compounds: II. Methylation of phenanthrene and alkylphenanthrenes. *Geochim. Cosmochim. Acta* **59**, 4259-4266.

Brocks J. J. and Schaeffer P. (2008) Okenane, a biomarker for purple sulfur bacteria (Chromatiaceae), and other new carotenoid derivatives from the 1640 Ma Barney Creek Formation. *Geochim. Cosmochim. Acta* **72**, 1396-1414.

547 Brocks J. J., Love G. D., Summons R. E., Knoll A. H., Logan G. A. and
548 Bowden S. A. (2005) Biomarker evidence for green and purple sulphur
549 bacteria in a stratified Palaeoproterozoic sea. *Nature* **437**, 866-870.
550 Brothers L., Engel M. H. and Krooss B. M. (1991) The effects of fluid flow
551 through porous media on the distribution of organic compounds in a
552 synthetic crude oil. *Org. Geochem.* **17**, 11-24.
553 Bull S. W. (1998) Sedimentology of the Palaeoproterozoic Barney Creek
554 formation in DDH BMR McArthur 2, southern McArthur basin,
555 Northern Territory. *Aust. J. Earth Sci.* **45**, 21-31.
556 Chen J., Walter M. R., Logan G. A., Hinman M. C. and Summons R. E.
557 (2003) The Paleoproterozoic McArthur River (HYC) Pb/Zn/Ag deposit of
558 northern Australia: organic geochemistry and ore genesis. *Earth*
559 *Planet. Sci. Lett.* **210**, 467-479.
560 Cooke D. R., Bull S. W., Large R. R. and McGoldrick P. J. (2000) The
561 importance of oxidized brines for the formation of Australian
562 Proterozoic stratiform sediment-hosted Pb-Zn (sedex) deposits. *Econ.*
563 *Geol.* **95**, 1-18.
564 Croxford N. J. W. (1968) A mineralogical examination of the McArthur lead-
565 zinc-silver deposit. *Proc. Aus. Inst. Min. Metall.* **226**, 97-108.
566 Dembicki Jr H., Meinschein W. G. and Hattin D. E. (1976) Possible
567 ecological and environmental significance of the predominance of even-
568 carbon number C20-C30 n-alkanes. *Geochim. Cosmochim. Acta* **40**,
569 203-208.

570 Dick J. M., Evans K. A., Holman A. I., Jaraula C. M. B. and Grice K. (2013)
571 Estimation and application of the thermodynamic properties of
572 aqueous phenanthrene and isomers of methylphenanthrene at high
573 temperature. *Geochim. Cosmochim. Acta* **122**, 247-266.
574 Garrigues P., Oudin J. L., Parlanti E., Monin J. C., Robcis S. and Bellocq J.
575 (1990) Alkylated phenanthrene distribution in artificially matured
576 kerogens from Kimmeridge clay and the Brent Formation (North Sea).
577 *Org. Geochem.* **16**, 167-173.
578 George S. C. and Ahmed M. (2002) Use of aromatic compound distributions
579 to evaluate organic maturity of the Proterozoic middle Velkerri
580 Formation, McArthur Basin, Australia. In *The Sedimentary Basins of*
581 *Western Australia 3: Proceedings of the Petroleum Exploration Society*
582 *of Australia Symposium 2002* (eds. M. Keep and S. J. Moss). Petroleum
583 Exploration Society of Australia, Perth. pp. 253-270.
584 George S. C., Llorca S. M. and Hamilton P. J. (1994) An integrated
585 analytical approach for determining the origin of solid bitumens in the
586 McArthur Basin, northern Australia. *Org. Geochem.* **21**, 235-248.
587 Grice K., Nabbefeld B. and Maslen E. (2007) Source and significance of
588 selected polycyclic aromatic hydrocarbons in sediments (Hovea-3 well,
589 Perth Basin, Western Australia) spanning the Permian-Triassic
590 boundary. *Org. Geochem.* **38**, 1795-1803.
591 Grice K., Cao C., Love G. D., Böttcher M. E., Twitchett R. J., Grosjean E.,
592 Summons R. E., Turgeon S. C., Dunning W. and Jin Y. (2005) Photic

zone euxinia during the Permian-Triassic superanoxic event. *Science* **307**, 706-709.

Grice K., Lu H., Atahan P., Asif M., Hallmann C., Greenwood P. F., Maslen E., Tulipani S., Williford K. and Dodson J. (2009) New insights into the origin of perylene in geological samples. *Geochim. Cosmochim. Acta* **73**, 6531-6543.

Grosjean E. and Logan G. A. (2007) Incorporation of organic contaminants into geochemical samples and an assessment of potential sources: examples from Geoscience Australia marine survey S282. *Org. Geochem.* **38**, 853-869.

Han J. and Calvin M. (1969) Hydrocarbon distribution of algae and bacteria, and microbiological activity in sediments. *Proc. Natl. Acad. Sci. U.S.A.* **64**, 436-443.

Holman A. I., Grice K., Jaraula C. M. B., Schimmelmann A. and Brocks J. J. (2012) Efficiency of extraction of polycyclic aromatic hydrocarbons from the Paleoproterozoic Here's Your Chance Pb/Zn/Ag ore deposit and implications for a study of Bitumen II. *Org. Geochem.* **52**, 81-87.

Ireland T., Bull S. W. and Large R. R. (2004a) Mass flow sedimentology within the HYC Zn-Pb-Ag deposit, Northern Territory, Australia: evidence for syn-sedimentary ore genesis. *Miner. Deposita* **39**, 143-158.

Ireland T., Large R. R., McGoldrick P. and Blake M. (2004b) Spatial distribution patterns of sulfur isotopes, nodular carbonate, and ore

615 textures in the McArthur River (HYC) Zn-Pb-Ag deposit, Northern
616 Territory, Australia. *Econ. Geol.* **99**, 1687-1709.
617 Kawka O. E. and Simoneit B. R. T. (1990) Polycyclic aromatic hydrocarbons
618 in hydrothermal petroleums from the Guaymas Basin spreading
619 center. *Appl. Geochem.* **5**, 17-27.
620 Ladygina N., Dedyukhina E. G. and Vainshtein M. B. (2006) A review on
621 microbial synthesis of hydrocarbons. *Process Biochem.* **41**, 1001-1014.
622 Large R. R., Bull S. W., McGoldrick P. J., Walters S., Derrick G. M. and
623 Carr G. R. (2005) Stratiform and strata-bound Zn-Pb-Ag deposits in
624 Proterozoic sedimentary basins, Northern Australia. In *Economic*
625 *Geology 100th Anniversary Volume* (eds. J. W. Hedenquist, J. F. H.
626 Thompson, R. J. Goldfarb and J. P. Richards). Society of Economic
627 Geologists, Littleton, Colorado. pp. 931-963.
628 Logan G. A., Hayes J. M., Hieshima G. B. and Summons R. E. (1995)
629 Terminal Proterozoic reorganization of biogeochemical cycles. *Nature*
630 **376**, 53-56.
631 Logan G. A., Hinman M. C., Walter M. R. and Summons R. E. (2001)
632 Biogeochemistry of the 1640 Ma McArthur River (HYC) lead-zinc ore
633 and host sediments, Northern Territory, Australia. *Geochim.*
634 *Cosmochim. Acta* **65**, 2317-2336.
635 Logan G. A., Calver C. R., Gorjan P., Summons R. E., Hayes J. M. and
636 Walter M. R. (1999) Terminal Proterozoic mid-shelf benthic microbial

637 mats in the Centralian Superbasin and their environmental
638 significance. *Geochim. Cosmochim. Acta* **63**, 1345-1358.
639 Londry K. L., Jahnke L. L. and Des Marais D. J. (2004) Stable carbon
640 isotope ratios of lipid biomarkers of sulfate-reducing bacteria. *Appl.*
641 *Environ. Microbiol.* **70**, 745-751.
642 Lyons T. W., Gellatly A. M., McGoldrick P. J. and Kah L. C. (2006)
643 Proterozoic sedimentary exhalative (SEDEX) deposits and links to
644 evolving global ocean chemistry. *Geol. Soc. Am. Mem.* **198**, 169-184.
645 Madigan M. T., Takigiku R., Lee R. G., Gest H. and Hayes J. M. (1989)
646 Carbon isotope fractionation by thermophilic phototrophic sulfur
647 bacteria: evidence for autotrophic growth in natural populations. *Appl.*
648 *Environ. Microbiol.* **55**, 639-644.
649 Marzi R., Torkelson B. E. and Olson R. K. (1993) A revised carbon
650 preference index. *Org. Geochem.* **20**, 1303-1306.
651 McCollom T. M., Simoneit B. R. T. and Shock E. L. (1999) Hydrous pyrolysis
652 of polycyclic aromatic hydrocarbons and implications for the origin of
653 PAH in hydrothermal petroleum. *Energy Fuels* **13**, 401-410.
654 McGoldrick P., Winefield P., Bull S., Selley D. and Scott R. (2010)
655 Sequences, synsedimentary structures, and sub-basins: the where and
656 when of SEDEX zinc systems in the southern McArthur Basin,
657 Australia. In *The Challenge of Finding New Mineral Resources: Global*
658 *Metallogeny, Innovative Exploration, and New Discoveries. Volume II:*
659 *Zinc-Lead, Nickel-Copper-PGE, and Uranium* (eds. R. J. Goldfarb, E.

E. Marsh and T. Monecke). Society of Economic Geologists Special Publication Number 15, Littleton, Colorado. pp. 367-389.

Melendez I., Grice K., Trinajstic K., Ladjavardi M., Greenwood P. and Thompson K. (2013) Biomarkers reveal the role of photic zone euxinia in exceptional fossil preservation: an organic geochemical perspective. *Geology* **41**, 123-126.

Nabbefeld B., Grice K., Summons R. E., Hays L. E. and Cao C. (2010a) Significance of polycyclic aromatic hydrocarbons (PAHs) in Permian/Triassic boundary sections. *Appl. Geochem.* **25**, 1374-1382.

Nabbefeld B., Grice K., Schimmelmann A., Summons R. E., Troitzsch U. and Twitchett R. J. (2010b) A comparison of thermal maturity parameters between freely extracted hydrocarbons (Bitumen I) and a second extract (Bitumen II) from within the kerogen matrix of Permian and Triassic sedimentary rocks. *Org. Geochem.* **41**, 78-87.

Page R. W. and Sweet I. P. (1998) Geochronology of basin phases in the western Mt Isa Inlier, and correlation with the McArthur Basin. *Aust. J. Earth Sci.* **45**, 219-232.

Planavsky N. J., McGoldrick P., Scott C. T., Li C., Reinhard C. T., Kelly A. E., Chu X., Bekker A., Love G. D. and Lyons T. W. (2011) Widespread iron-rich conditions in the mid-Proterozoic ocean. *Nature* **477**, 448-451.

Poulton S. W., Fralick P. W. and Canfield D. E. (2010) Spatial variability in oceanic redox structure 1.8 billion years ago. *Nat. Geosci.* **3**, 486-490.

682 Powell T. G., Jackson M. J., Sweet I. P., Crick I. H., Boreham C. J. and
683 Summons R. E. (1987) Petroleum geology and geochemistry, Middle
684 Proterozoic McArthur Basin. Australia Bureau of Mineral Resources,
685 Geology and Geophysics, record 1987/48.
686 Püttmann W., Merz C. and Speczik S. (1989) The secondary oxidation of
687 organic material and its influence on Kupferschiefer mineralization of
688 southwest Poland. *Appl. Geochem.* **4**, 151-161.
689 Radke M., Willsch H., Leythaeuser D. and Teichmüller M. (1982) Aromatic
690 components of coal: relation of distribution pattern to rank. *Geochim.*
691 *Cosmochim. Acta* **46**, 1831-1848.
692 Řezanka T., Sokolov M. Y. and Víden I. (1990) Unusual and very-long-chain
693 fatty acids in Desulfotomaculum, a sulfate-reducing bacterium. *FEMS*
694 *Microbiol. Lett.* **73**, 231-237.
695 Robl T. L. and Davis B. H. (1993) Comparison of the HF-HCl and HF-BF3
696 maceration techniques and the chemistry of resultant organic
697 concentrates. *Org. Geochem.* **20**, 249-255.
698 Sherman L. S., Waldbauer J. R. and Summons R. E. (2007) Improved
699 methods for isolating and validating indigenous biomarkers in
700 Precambrian rocks. *Org. Geochem.* **38**, 1987-2000.
701 Simoneit B. R. T. (1994) Lipid/bitumen maturation by hydrothermal activity
702 in sediments of Middle Valley, Leg 139. In *Proceedings of the Ocean*
703 *Drilling Program, Scientific Results, Vol. 139* (eds. M. J. Mottl, E. E.

Davis, A. T. Fisher and J. F. Slack). Ocean Drilling Program, College Station, Texas. pp. 447-465.

Stein S. E. (1978) On the high temperature chemical equilibria of polycyclic aromatic hydrocarbons. *J. Phys. Chem.* **82**, 566-571.

Summons R. E. and Powell T. G. (1987) Identification of aryl isoprenoids in source rocks and crude oils: biological markers for the green sulphur bacteria. *Geochim. Cosmochim. Acta* **51**, 557-566.

Summons R. E., Powell T. G. and Boreham C. J. (1988) Petroleum geology and geochemistry of the Middle Proterozoic McArthur Basin, Northern Australia: III. Composition of extractable hydrocarbons. *Geochim. Cosmochim. Acta* **52**, 1747-1763.

Szczerba M. and Rospondek M. J. (2010) Controls on distributions of methylphenanthrenes in sedimentary rock extracts: critical evaluation of existing geochemical data from molecular modelling. *Org. Geochem.* **41**, 1297-1311.

Theng B. K. G., Aislabie J. and Fraser R. (2001) Bioavailability of phenanthrene intercalated into an alkylammonium–montmorillonite clay. *Soil Biol. Biochem.* **33**, 845-848.

Vahrman M. and Watts R. H. (1972) The smaller molecules obtainable from coal and their significance: Part 6. Hydrocarbons from coal heated in thin layers. *Fuel* **51**, 235-241.

van Aarssen B. G. K., Bastow T. P., Alexander R. and Kagi R. I. (1999) Distributions of methylated naphthalenes in crude oils: indicators of maturity, biodegradation and mixing. *Org. Geochem.* **30**, 1213-1227.

Venkatesan M. I. and Dahl J. (1989) Organic geochemical evidence for global fires at the Cretaceous/Tertiary boundary. *Nature* **338**, 57-60.

Voigtmann M. F., Yang K., Batts B. D. and Smith J. W. (1994) Evidence for synthetic generation of methylphenanthrenes in sediments. *Fuel* **73**, 1899-1903.

Wakeham S. G., Schaffner C. and Giger W. (1980a) Polycyclic aromatic hydrocarbons in Recent lake sediments—II. Compounds derived from biogenic precursors during early diagenesis. *Geochim. Cosmochim. Acta* **44**, 415-429.

Wakeham S. G., Schaffner C. and Giger W. (1980b) Polycyclic aromatic hydrocarbons in Recent lake sediments—I. Compounds having anthropogenic origins. *Geochim. Cosmochim. Acta* **44**, 403-413.

Walker R. N., Logan R. G. and Binnekamp J. G. (1977) Recent geological advances concerning the H.Y.C. and associated deposits, McArthur River, N.T. *J. Geol. Soc. Aus.* **24**, 365-380.

Williford K. H., Grice K., Logan G. A., Chen J. and Huston D. (2011) The molecular and isotopic effects of hydrothermal alteration of organic matter in the Paleoproterozoic McArthur River Pb/Zn/Ag ore deposit. *Earth Planet. Sci. Lett.* **301**, 382-392.

748

Captions of tables and figures

Table 1

Average chain length (ACL) and carbon preference index (CPI) for Bitumen II *n*-alkanes, plus stable carbon isotope ratios ($\delta^{13}C$) of *n*-alkanes and isolated kerogen. $\delta^{13}C$ is given as the average of repeated analyses, with one standard deviation shown in parentheses and the number of analyses in superscript. CPI was calculated using the generalised formula of Marzi et al. (1993), with n = 7 and m = 17. WFS – W-Fold Shale unit.

Table 2

Quantification of selected PAHs present in Bitumen II aromatic fractions, plus calculated PAH ratios for Bitumens I and II. Bitumen I ratios were calculated from data presented by Williford et al. (2011).

Figure 1

Structures of PAHs discussed in the text. Positions of methylation are indicated for phenanthrene. Equations of the methylphenanthrene index (MPI-1) and methylphenanthrene ratio (MPR) are taken from (Radke et al., 1982).

Figure 2

Total ion chromatograms of (A) pit 1 Bitumen II saturate fraction, (B) pit 3 Bitumen II saturate fraction and (C) pit 1 Bitumen II aromatic fraction. *n*-Alkanes in (A) and (B) are marked with open circles and even carbon numbers are labelled. Labels in (C) are a: phenanthrene, b: methylphenanthrenes, c: pyrene, d: chrysene + triphenylene, e: benzo[*e*]pyrene, f: benzo[*ghi*]perylene and g: coronene.

Figure 3

$\delta^{13}C$ of *n*-alkanes from Bitumens I (carbon number range C_{18} to C_{21}), Bitumen II (ranges C_{16} + C_{18} and C_{24} to C_{32}) and bulk $\delta^{13}C$ of isolated kerogen from HYC sample pits. Bitumen I data was taken from Williford et al. (2011). Error bars are one standard deviation.

Figure 4

Selected PAH ratios calculated for Bitumens I and II. (A) methylphenanthrene index (MPI-1) and (B) methylphenanthrene ratio (MPR). Equations of MPI-1 and MPR are shown in Fig. 1. Bitumen I data was taken from Williford et al. (2011).

Figure 5

Relative proportion of phenanthrene (P) and methylphenanthrenes (MP) for (A) Bitumen I and (B) Bitumen II. Bitumen I data was taken from Williford et al. (2011).

Table 1

	Pit 1	Pit 2	Pit 3	Pit 4	Pit 5	WFS
Distance from pit 1 (m)	0	104	372	553	710	-
Molecular parameters						
ACL	26.3	26.9	26.7	25.6	25.4	25.6
CPI	0.67	0.91	0.98	0.94	0.83	0.59
$\delta^{13}C$ (‰)						
C_{16} + C_{18}	-32.2 (0.3)[5]	-	-32.5 (0.2)[2]	-32.1 (0.4)[4]	-32.4 (0.3)[2]	-31.6 (0.5)[4]
C_{24}-C_{32}	-32.3 (0.3)[5]	-31.7 (0.2)[2]	-34.2 (0.2)[2]	-34 (0.3)[4]	-33.4 (0.5)[2]	-34.4 (0.5)[4]
Kerogen	-35.5 (0.1)	-36.3 (0.1)	-35.6 (0.1)	-37.0 (0.1)	-34.2 (0.1)	-35.5 (0.1)

Table 2

	Pit 1	Pit 2	Pit 3	Pit 4	Pit 5	WFS
Compounds (ppb/TOC)						
Phenanthrene	615	327	379	1156	334	231
3-Methylphenanthrene	424	190	263	754	232	249
2-Methylphenanthrene	479	283	339	948	274	250
9-Methylphenanthrene	358	181	247	616	243	277
1-Methylphenanthrene	358	174	260	689	263	315
Pyrene	391	192	156	558	160	202
Chrysene	327	125	356	481	273	477
Benzo[e]pyrene	772	180	830	490	658	1025
Benzo[ghi]perylene	358	111	266	185	254	317
Coronene	101	-	57	-	42	27
Bitumen I PAH ratios						
MPI-1	1.02	1.04	1.02	1.04	0.90	0.91
MPR	1.34	1.62	1.31	1.38	1.04	0.79
MP/P	2.63	2.53	2.93	2.60	3.03	4.72
BePyr/Pyr	1.97	0.94	5.33	0.88	4.11	5.08
BePyr/Chry	2.36	1.44	2.33	1.02	2.41	2.15
Chry/Phen	0.53	0.38	0.94	0.42	0.82	2.06
BePery/Phen	0.58	0.34	0.70	0.16	0.76	1.37
BePery/Pyr	0.92	0.58	1.71	0.33	1.59	1.57
BePery/Chry	1.09	0.89	0.75	0.38	0.93	0.66
BePery/BePyr	0.46	0.61	0.32	0.38	0.39	0.31
Bitumen I PAH ratios						
MPI-1	1.38	1.41	1.26	1.49	1.34	1.25
MPR	1.37	1.32	1.21	1.35	1.12	1.26
MP/P	5.00	6.26	5.31	7.05	9.32	4.67

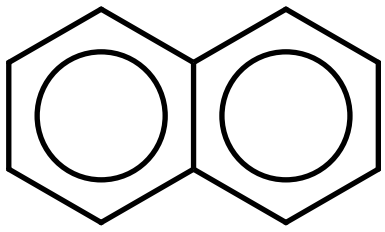

naphthalene

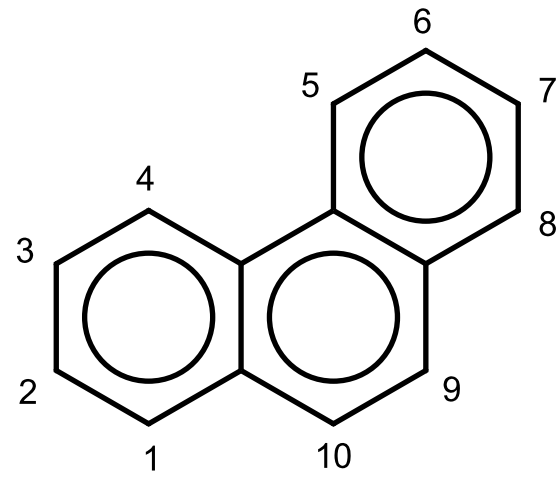

phenanthrene (P)

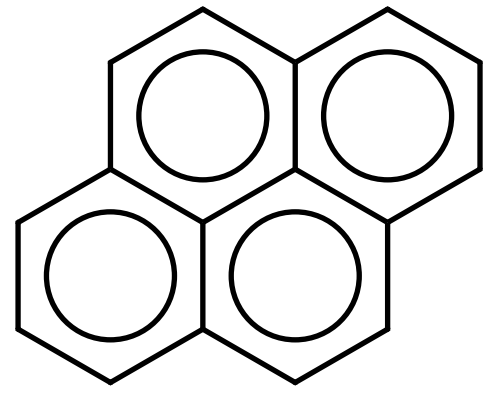

pyrene

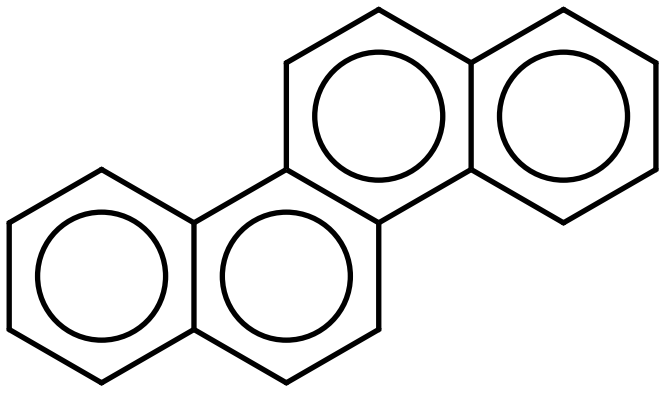

chrysene

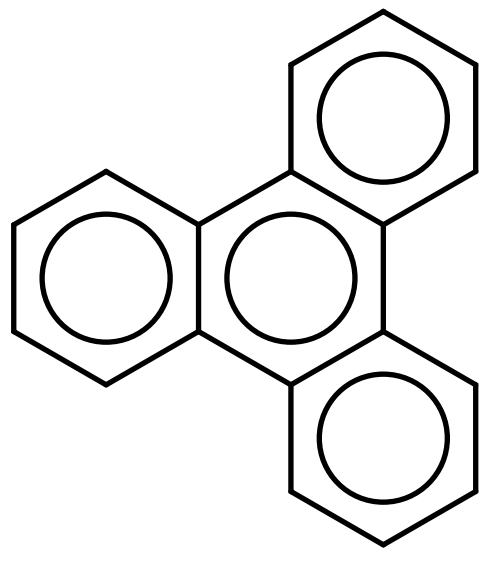

triphenylene

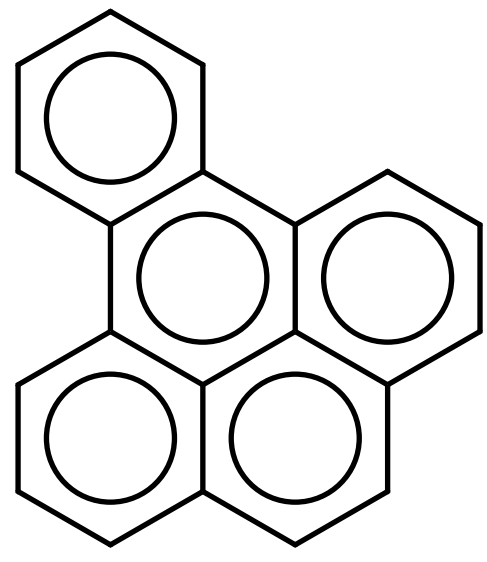

benzo[e]pyrene

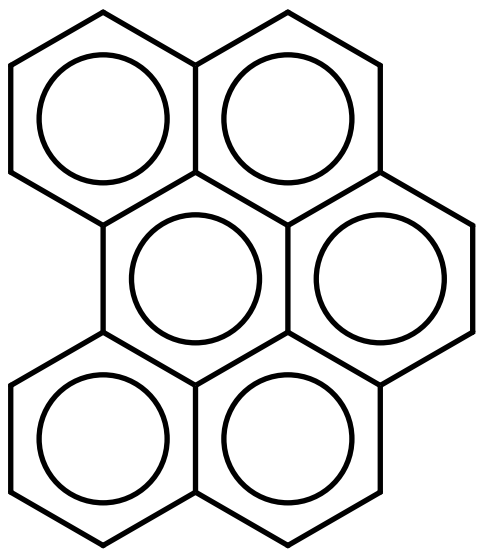

benzo[ghi]perylene

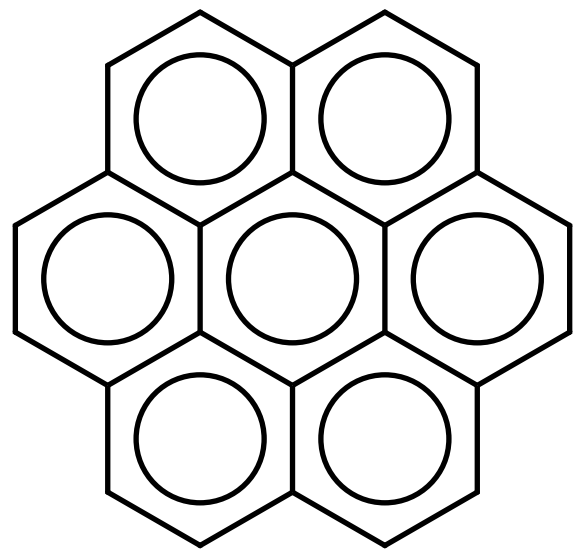

coronene

$$\text{MPI-1} = 1.5\ \frac{\text{2-MP} + \text{3-MP}}{\text{P} + \text{1-MP} + \text{9-MP}} \qquad \text{MPR} = \frac{\text{2-MP}}{\text{1-MP}}$$

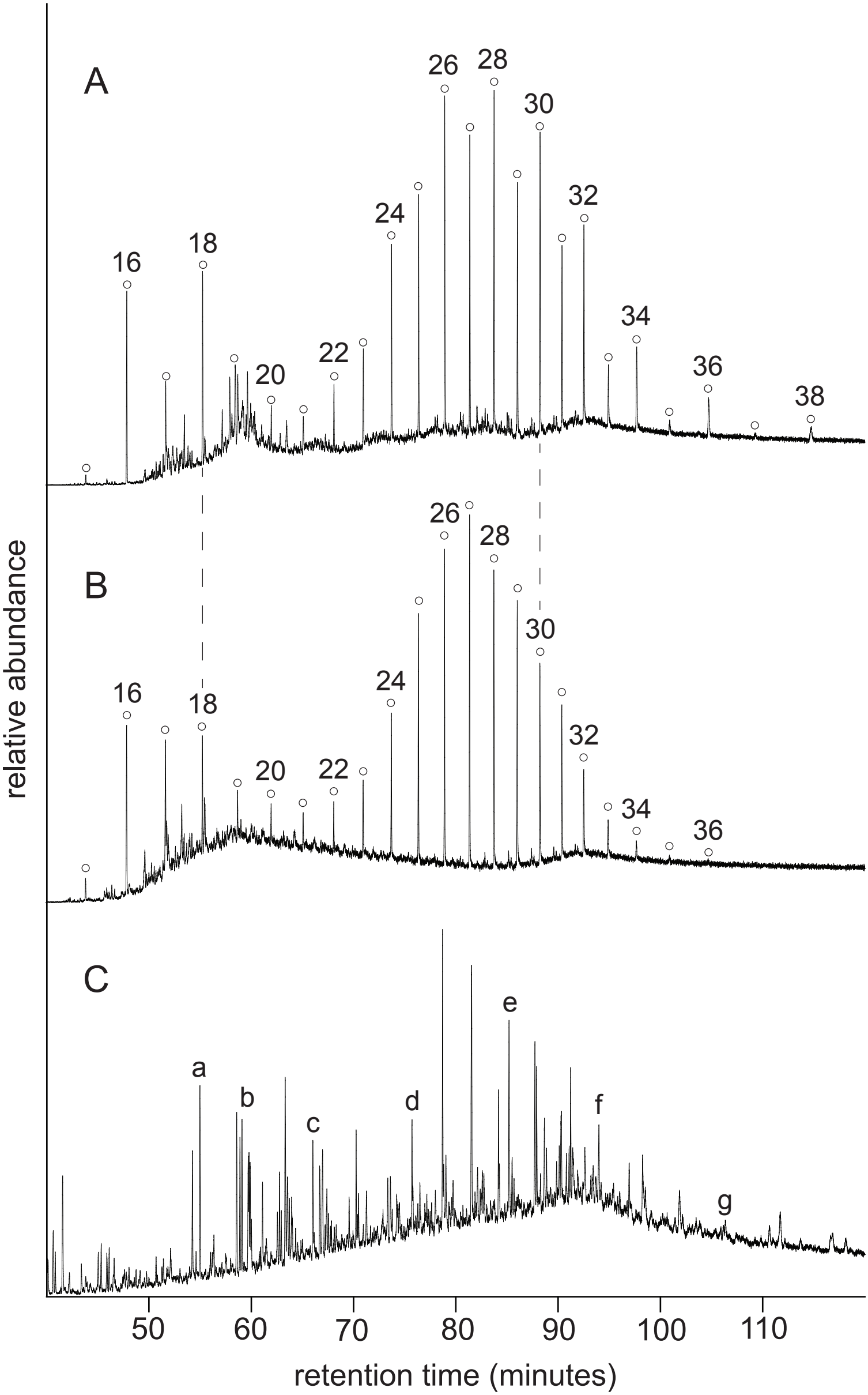
A
16
18
20
22
24
26
28
30
32
34
36
38
B
16
18
20
22
24
26
28
30
32
34
36
C
a
b
c
d
e
f
g
relative abundance
50
60
70
80
90
100
110
retention time (minutes)

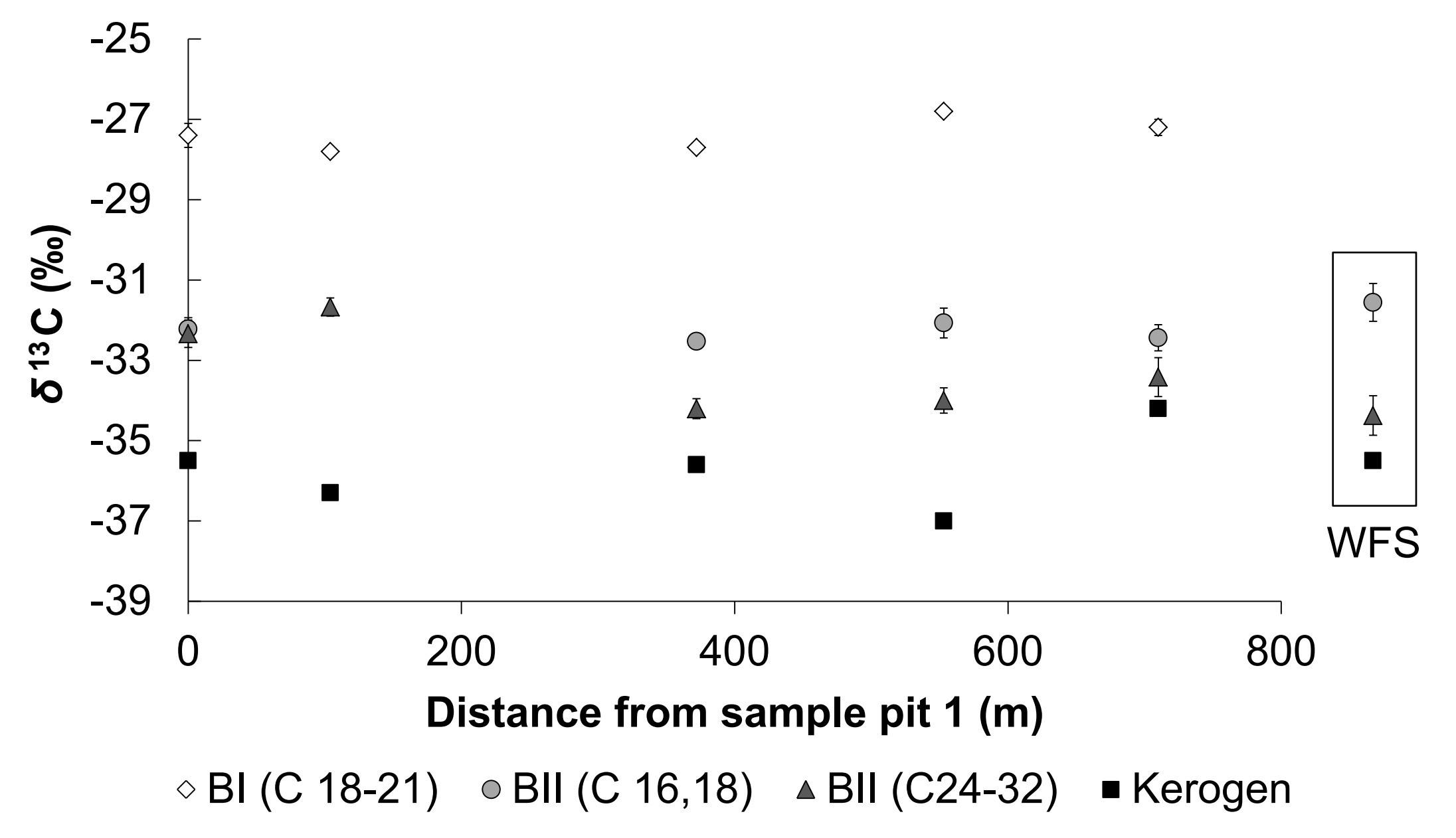
-25
-27
-29
-31
-33
-35
-37
-39
δ13C (‰)
0
200
400
600
800
Distance from sample pit 1 (m)
WFS
BI (C 18-21)
BII (C 16,18)
BII (C24-32)
Kerogen

A

MPI-1

1.6
1.4
1.2
1
0.8
0.6

0
200
400
600
800

Distance from sample pit 1 (m)

WFS

B

MPR

1.8
1.6
1.4
1.2
1
0.8
0.6

0
200
400
600
800

Distance from sample pit 1 (m)

WFS

◇ Bitumen I ■ Bitumen II

A

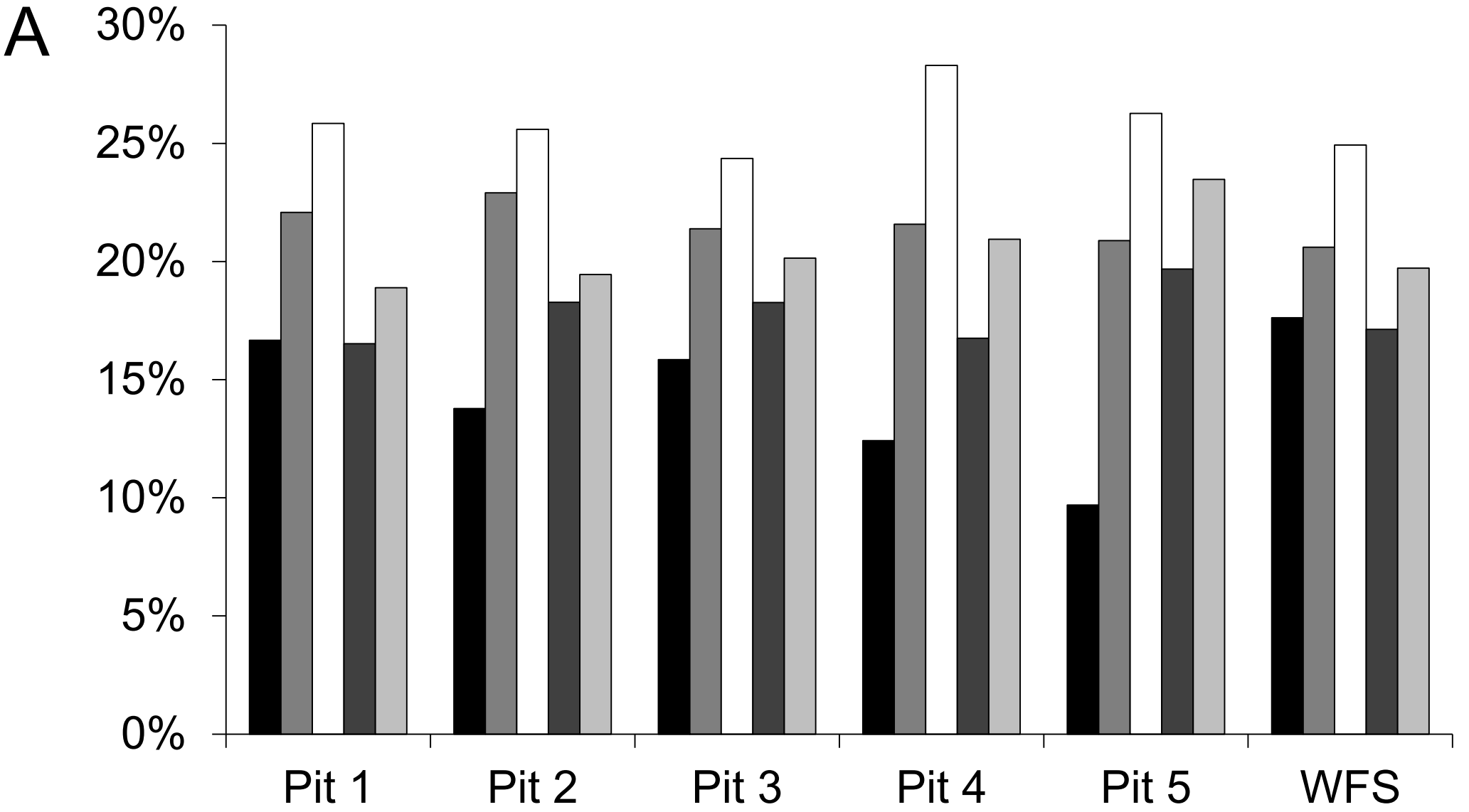
30%
25%
20%
15%
10%
5%
0%
Pit 1
Pit 2
Pit 3
Pit 4
Pit 5
WFS

B

30%
25%
20%
15%
10%
5%
0%
Pit 1
Pit 2
Pit 3
Pit 4
Pit 5
WFS
P
3-MP
2-MP
9-MP
1-MP